UDK 669.721.5:621.791.763:52-334.2
Original scientific article/Izvirni znanstveni članek

ISSN 1580-2949
Mater. Tehnol.

PREPARATION OF Mg-7Sn-1Ca MAGNESIUM ALLOY AND STUDY OF ITS RESISTANCE SPOT WELDING MICROSTRUCTURE AND MECHANICAL PROPERTIES

PRIPRAVA MAGNEZIJEVE ZLITINE TIPA MG-7SN-1CA TER ŠTUDIJ MIKROSTRUKTURE IN MEHANSKIH LASTNOSTI UPOROVNO TOČKOVNO VARJENIH SPOJEV

Xinyu Xu, Jing Hu, Zheng Jia*

School of Mechanical Engineering, Shenyang University, Shenyang 110044

Prejem rokopisa – received: 2024-10-20; sprejem za objavo – accepted for publication: 2025-02-17

doi:10.17222/mit.2024.1331

This paper investigated a 1.5-mm-thick Mg-7Sn-1Ca magnesium alloy through resistance spot welding, examining how the welding current affects the joint microstructure, nugget diameter and tensile strength. Various experimental techniques, including tensile tests, microhardness testing, optical microscopy, and scanning electron microscopy, were employed for a detailed analysis. The optimal mechanical performance was achieved under conditions of 14 kA current, 1 kN pressure, and 0.4 s welding time, with a tensile strength of 1.0295 kN and nugget diameter of 2.25 mm. The welded joints mainly consist of a nugget zone and a heat-affected zone. The nugget zone exhibits the highest microhardness, significantly exceeding that of the heat-affected zone and the base metal. The nugget zone is primarily composed of equiaxed dendrites and columnar dendrites, with grain coarsening observed in both the nugget and heat-affected zones. The microstructural features, fracture-surface morphology, and microhardness distribution of the joints were thoroughly investigated. These analyses provide valuable data on joint performance, aiding in the further understanding and optimization of the welding process.

Key words: magnesium alloys, resistance spot welding, welded joints, mechanical properties, microstructure

V članku avtorji opisujejo raziskavo uporovno točkovnega varjenja 1,5 mm debele pločevine iz magnezijeve zlitine tipa Mg-7Sn-1Ca. Raziskovalci so analizirali predvsem kako električni tok varjenja vpliva na mikrostrukturo nastalih zvarov, njihov premer in natezno trdnost. Pri tem so za natančne analize uporabili različne eksperimentalne tehnike, kot so: natezni preizkus, prizkus določitve mikrotrdote, optično in elektronsko vrstično mikroskopijo. Optimalne mehanske lastnosti zvarnih spojev so dosegli pri električnem toku varjenja 14 kA, tlaku 1 kN in času 0,4 sekunde. Pri teh procesnih parametrih je bila natezna trdnost spojev enaka 10295 kN in premer zvarov v obliki »lešnikov« 2,25 mm. Zvarni spoji so bili v glavnem sestavljeni iz cone, kjer je prišlo do taljenja (angl.: nugget zone) in toplotno vplivane cone (angl.: heat-affected zone). Prva od obeh con je imela najvišjo mikrotrdoto. Ta je bila precej višja od mikrotrdote osnovnega materiala in mikrotrdote toplotno vplivane cone. Cona v obliki »lešnikov« je bila sestavljena predvsem iz grobih enoosnih in stebričastih dendritov. Toplotno vplivana cona je imela prav tako grobo mikrozrnato mikrostrukturo. Avtorji pričujoče raziskave so detajlno analizirali mikrostrukturne značilnosti, morfologijo prelomov in porazdelitev mikrotrdote po preseku zvarnih spojev. V tem članku avtorji povdarjajo, da je ta raziskava pripomogla k boljšemu razumevanju, pridobitvi relevantnih podatkov in optimiziranju procesa uporovnega točkovnega varjenja zlitin na osnovi Mg.

Ključne besede: magnezijeve zlitine, uporovno točkovno varjenje, zvarni spoji, mehanske lastnosti, mikrostruktura

1 INTRODUCTION

Magnesium alloys, due to their light weight and high strength, have broad application prospects in various fields.[1] Nevertheless, issues such as low absolute strength, poor corrosion resistance, and insufficient plasticity significantly restrict their broader application. In the current global context of energy conservation and emission reduction, developing new types of magnesium alloys is particularly important. Exiting research shows that adding rare-earth elements can improve the performance of magnesium alloys at both room and high temperatures.[2] However, traditional magnesium alloys often contain rare-earth elements, which increases costs and places environmental pressure due to their high prices. This makes their large-scale application challenging. Therefore, developing rare-earth-free, high-performance magnesium alloys is crucial. In this context, Mg-Sn alloys are gaining attention for their unique advantages, including excellent high-temperature stability, significant solid-solution strengthening potential, and strong creep resistance. Additionally, Mg-Sn alloys are cost-effective, and the grain-refinement effect is stronger when both Sn and Ca are added compared to when they are added individually. The combined effect of Sn and Ca can lead to different outcomes than when added separately. Thus, adding Ca to Mg-Sn alloys not only improves high-temperature resistance but also enhances mechanical properties through the combined refinement effect of Ca and Sn. Furthermore, resistance spot welding, known for its

*Corresponding author's e-mail:
jz140@163.com (Zheng Jia)

speed and efficiency, is widely used in various fields, including electronics, aerospace, automotive, and everyday products.[3] With technological advancements, the intelligence and automation of resistance spot welding are expected to improve, providing a solid foundation for industrial development.[4] This offers new ideas for developing rare-earth-free, high-performance magnesium alloys and is expected to expand their application. The future of resistance spot welding will rely more on advanced control systems and precise sensors for automatic monitoring, intelligent adjustment, and optimization, significantly improving welding efficiency and quality. This innovation is expected to lower production costs and enhance the widespread use of magnesium alloys in fields like electronics and rail transportation, contributing to sustainable development. The goal of this research is to investigate the impact of welding process parameters on the performance of Mg-7Sn-1Ca magnesium alloy welds, providing a theoretical basis for determining the optimal welding method for magnesium alloys by comparing mechanical properties and microstructures under different parameters.

2 EXPERIMENTAL METHODS

In this experiment, high-purity industrial raw materials were used to prepare a Mg-7Sn-1Ca alloy. The Mg-7Sn-1Ca alloy was selected as the research material, and resistance spot welding was performed to study the mechanical properties and microstructure of the spot welds. Specifically, industrial-grade pure Mg (with a purity of 99.9 *w*/%) and pure Sn (with a purity of 99.9 *w*/%) were used in the alloy preparation. During the magnesium alloy preparation process, special consideration was given to the burn-off of pure Mg during melting, so a 3 % burn-off allowance was reserved to ensure the accurate content of Mg in the final alloy. For other alloying elements, Sn and Ca, the recovery rate was calculated as 100 % to ensure an accurate alloy composition. Through this scientific ratio and accurate calculation, the experiment successfully produced the expected Mg-7Sn-1Ca alloy.

In this experiment, Yaskawa robots were used for operating the spot-welding process. The servo welding gun electrodes were responsible for applying current and pressure. Under an electrode pressure of 1 kN and welding time of 0.4 s, three sets of samples were welded with welding currents of 12 kA, 14 kA, and 16 kA. During the tensile testing of the resistance spot weld lap specimens, the samples were primarily subjected to shear forces, a test known as shear testing. The core objective was to determine the maximum shear load of the specimens, which is a key parameter for evaluating the strength of the weld joints[5]. The experiment was repeated three times to enhance accuracy, with the equipment precisely controlling and recording force and displacement changes, and the stretching rate set at 1 mm/min to ensure reliable results. Microhardness testing was performed on the specimens using an HV-1000AZ Vickers hardness tester, with precise measurement and analysis of the microhardness in different regions of the weld joint. The loading conditions were set to a load of 1.962 N with a holding time of 15 s, and the interval between points was 0.2 mm. The experiment used high-purity industrial raw materials to prepare Mg-7Sn-1Ca alloy. The alloy was chosen for study and welded using resistance spot welding, focusing on the mechanical properties and microstructure of the weld joints. Specifically, industrial-grade Mg (99.9 *w*/% purity) and Sn (99.9 *w*/% purity) were used. A 3 % loss of Mg was accounted for during melting to ensure accurate Mg content, while Sn and Ca were assumed to have a 100 % yield. This careful composition led to the successful preparation of the Mg-7Sn-1Ca alloy.

The welding process was conducted using a Yaskawa robot with a servo welding gun applying current and pressure[6]. The welding was done with the electrode pressure set at 1 kN and a welding time of 0.4 s under currents of 12 kA, 14 kA, and 16 kA. The lap shear tests, which measure maximum shear load, were repeated three times for accuracy, with the test rate set at 1 mm/min. Microhardness tests were performed using an HV-1000AZ Vickers hardness tester, with specific load and pressure conditions. Detailed observations of the microstructures were conducted using an OLYMPUS metallographic microscope, focusing on the nugget zone, heat-affected zone, and base metal. Additionally, the SEM model S-4800 was used to examine the fracture morphology and distribution.

3 RESULTS

3.1 Analysis of the Microstructure and Mechanical Properties of Mg-7Sn-1Ca Magnesium Alloy

Under different currents of 12 kA, 14 kA, and 16 kA, the macro morphology of the spot weld joints observed under a low-magnification microscope is shown in **Figure 1**. These images clearly illustrate the impact of current variation on the morphology of the weld nugget.[7] As the welding current increases, the heat input during the welding process also increases, leading to a corresponding expansion in the size of the weld nugget. Significant changes in nugget diameter are observed with variations in welding current. At lower welding currents, the heat input is limited, resulting in slower and smaller nugget formation. As the welding current gradually increases, the heat input also rises, directly affecting the temperature distribution and melting rate in the welding area, there by significantly enlarging the nugget size.

However, it is important to note that when the current exceeds 14 kA and is further increased to 16 kA, excessive heating causes spatter in the nugget area (**Figure 1c**), which leads to cracks and pores in the nugget. The integrity of the nugget is compromised by metal

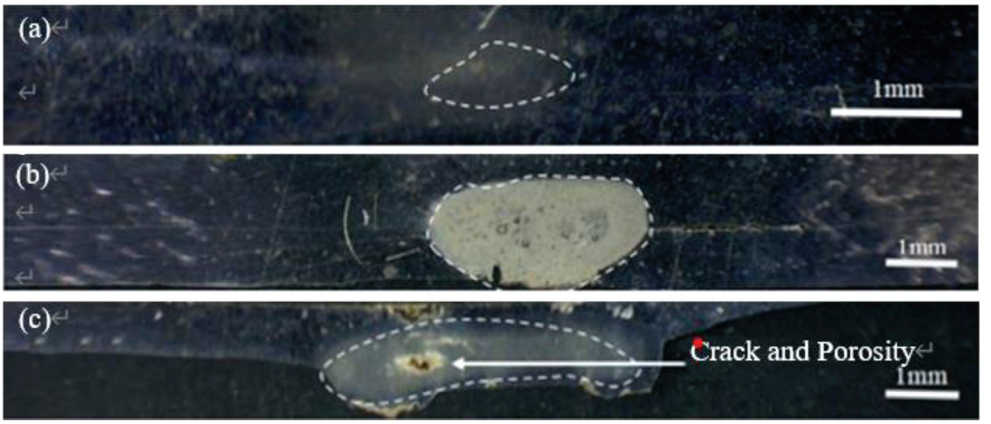

Figure 1: Macro appearance of spot welds at different currents: a) 12 kA, b) 14 kA, c) 16 kA

spatter, causing stress concentration at the nugget edges, which significantly reduces the mechanical properties of the joint. Moreover, metal spatter adversely affects the formation of the joint.[8] Metal spatter is undesirable in practical production as it negatively impacts the weld joint. In this experimental setting, it was found that the critical welding current for nugget spatter is 16 kA. To ensure process stability and quality, a slightly lower current, such as 14 kA, is recommended as the suitable welding current.

Figure 2 shows the microscopic structure of the nugget formed under different current conditions observed through an optical microscope (OM). The weld joint consists of three main parts: the base material, the heat-affected zone (HAZ), and the nugget zone. The nugget zone is the core area of the joint, further divided into the columnar dendrite zone (CDZ) and the equiaxed dendrite zone (EDZ) within the nugget.[9–13] This structure allows the weld joint to maintain high strength and stability under various external forces. The interaction and cooperation among these zones are also key factors in ensuring the performance of the weld joint. Therefore, when studying and optimizing weld joints, it is necessary to fully consider the characteristics and interactions of each component to achieve the best welding results. Regarding the impact of different welding currents on CDZ changes, experimental results show that under the influence of heat input, the grain size of the heat-affected zone has not changed significantly compared to the base material, mainly due to the high thermal conductivity of magnesium alloys. Notably, at a welding current of 12 kA, the CDZ zone is not evident in the figure due to the smaller nugget diameter. From **Figure 2a** to **2c** it can be observed that as the welding current gradually in-

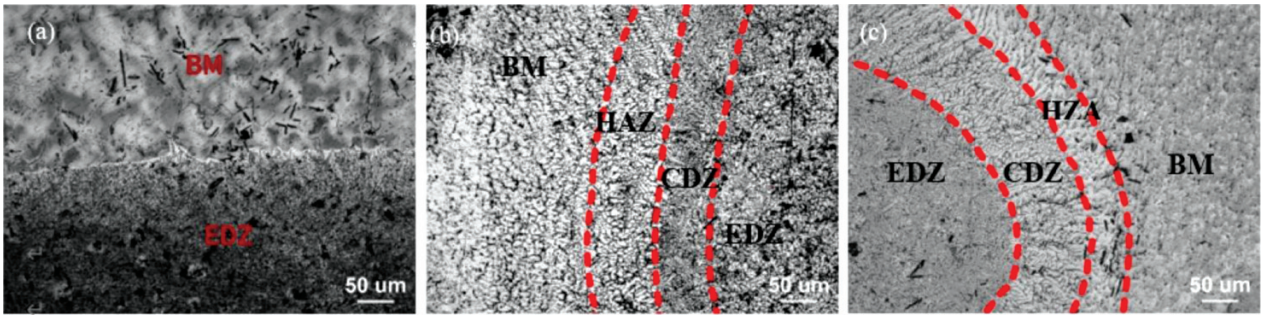

Figure 2: Microstructure changes under different welding currents: a) 12 kA, b) 14 kA, c) 16 kA

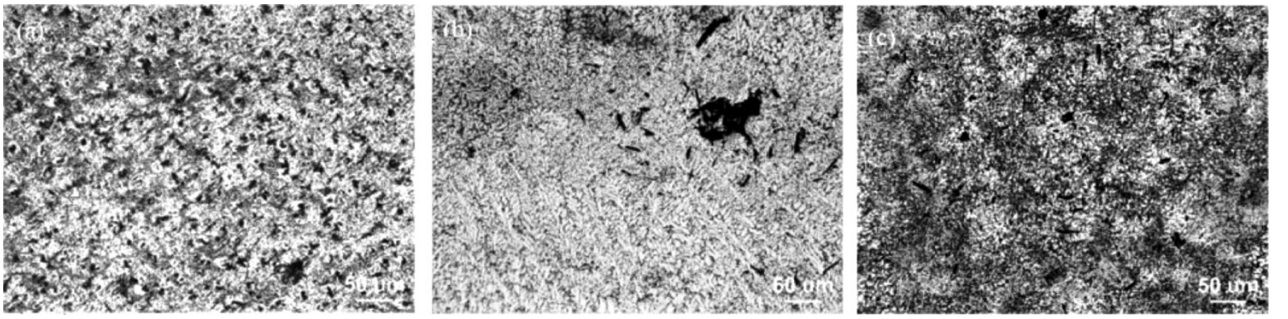

Figure 3: Changes in the nugget zone under different welding currents: a) 12 kA, b) 14 kA, c) 16 kA

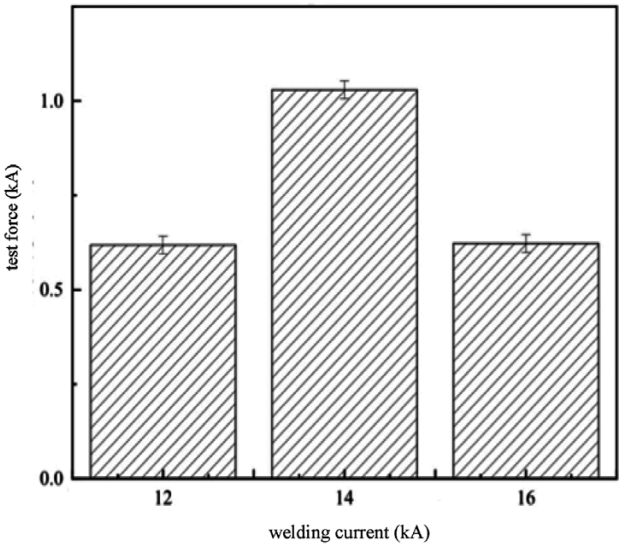

Figure 4: Variation of the peak values at 12 kA, 14 kA, and 16 kA currents

creases, the welding heat input also increases correspondingly. During this process, the CDZ formed in the NZ near the heat-affected zone shows a trend of narrowing. Additionally, under the welding current of 16 kA, the nugget line between NZ and HAZ becomes apparent, and the grain size difference between the two parts is significant. These phenomena arise from the structural characteristics of the alloy formed under compositional undercooling conditions.

Observing **Figure 3a** to **3c**, as the heat input gradually increases, the area affected by the latent heat released by each dendrite axis expnds.[14] This effect increases the width of the undercooled zone at the interface front, providing neighboring dendrite axes with the potential to grow further. As a result, the dendrite spacing increases, leading to coarsening of the microstructure, which is an important factor affecting the mechanical properties of the CDZ. Analyzing the microscopic transformation, with increased heat input, the cooling rate in the nugget zone slows down significantly, leading to a decrease in undercooling.[15] This series of thermodynamic changes ultimately affects the nucleation rate, causing a significant reduction. In summary, the increase in welding current affects the heat input and cooling rate, thereby altering the microstructure of the nugget. The originally fine equiaxed dendrite zone becomes coarser.

3.2 Mechanical properties of resistance spot welding joints

In the process of conducting tensile shear tests on three sets of samples to observe the impact of current on the joint's tensile performance, tensile strength data for the three sets of samples were obtained after the tests.[16–20] To present this data more intuitively, the average tensile strength values for the three sets of samples were calculated and organized into a bar chart, as shown in **Figure 4**. This bar chart clearly illustrates the tensile performance of the joints at different currents.

According to the chart, when the welding current is 14 kA, the tensile performance of the joint reaches its peak, with a tensile strength of 1.0295 kN. This indicates that at this current, the joint has the highest tensile strength and can withstand the maximum tensile load. However, when the current is increased to 16 kA, the tensile performance of the joint decreases to 0.6225 kN. This reduction is due to the overheating of the weld joint caused by excessively high current. The excessive heat input can lead to spattering of the molten metal, which not only reduces the amount of metal in the joint but also causes structural defects in the weld area, such as cracks or voids, significantly lowering the overall strength of the joint.[21] It can be further analyzed that when the welding current varies from 12 kA to 16 kA, the shear strength of the joint first increases and then decreases. Specifically, as the current increases, the shear strength gradually increases, reaching a peak value of 1.0295 kN when the welding current is 14 kA. After this point, the shear strength begins to decrease.[22] At lower welding currents, an insufficient heat input results in a smaller weld nugget, leading to weaker shear strength of the joint. However, as the welding current increases, the diameter of the weld nugget enlarges due to the increased internal heat source, thus improving the shear strength of the weld. But when the welding current exceeds 14 kA, excessive heating causes spattering (**Figure 1c**), which introduces cracks and pores in the weld nugget.

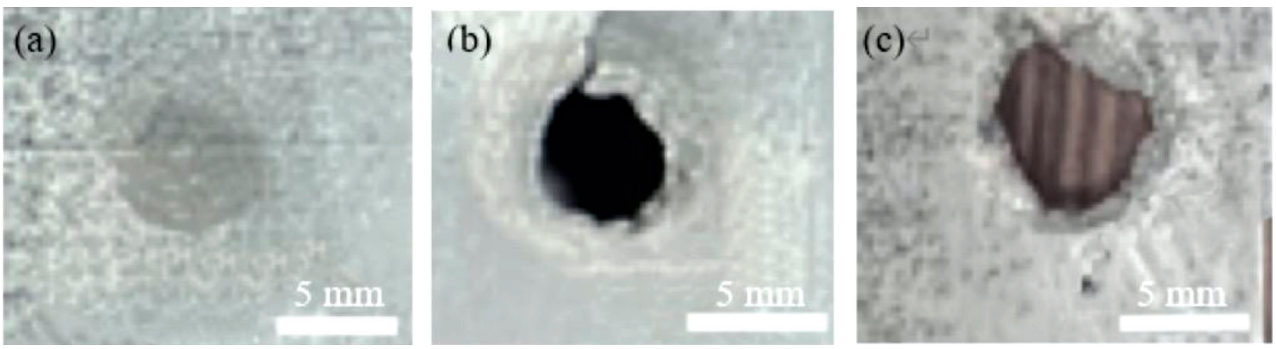

Figure 5: The macro appearance of the fracture: a) is interface failure, b), c) are pull-out failures

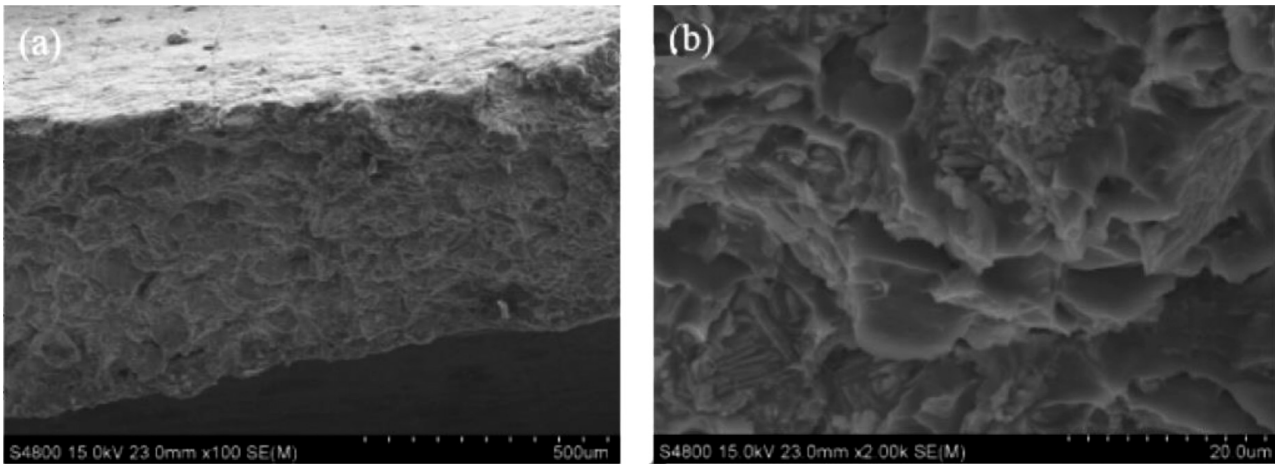

Figure 6: a) is the SEM scanning image of the fracture surface at a welding current of 12 kA, and b) is a magnified view of a region from (a)

Figure 5, through a comparative analysis of fracture morphologies under different failure modes, provides a deeper understanding of the formation mechanisms and characteristics of various failure modes.[23–25] This, in turn, offers theoretical support and practical guidance for optimizing resistance spot welding processes and improving weld quality. Interface failure typically starts from the center of the weld nugget and expands outward, leading to complete separation of the weld joint, as shown in **Figure 5a**. Weld nugget pull-out failure occurs when the nugget is pulled out from one side of the sheet, causing a loss of joint connectivity, as depicted in **Figures 5b** and

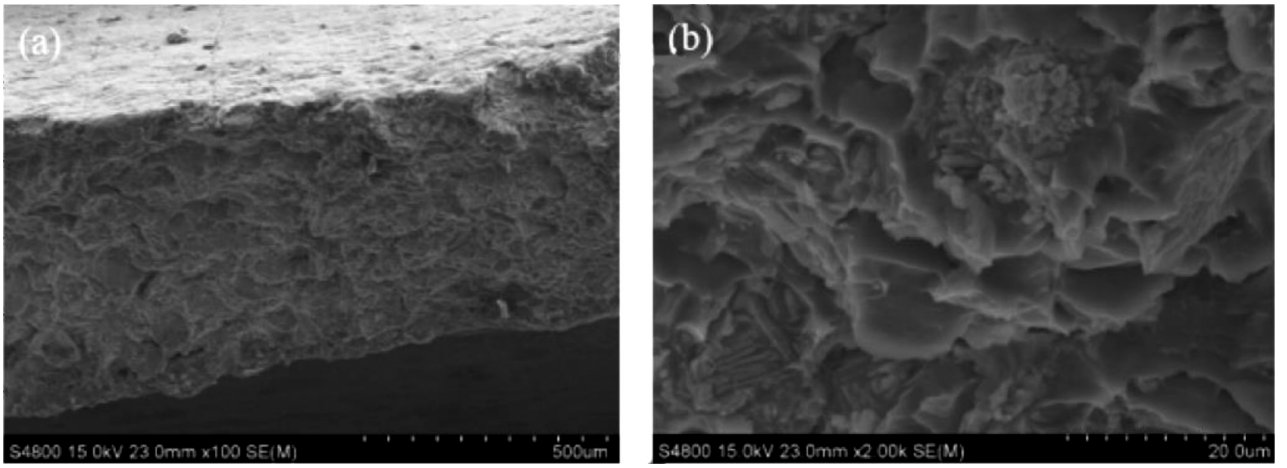

Figure 7: a) is the SEM scanning image of the fracture surface at a welding current of 14 kA, and b) is a magnified view of a region from (a)

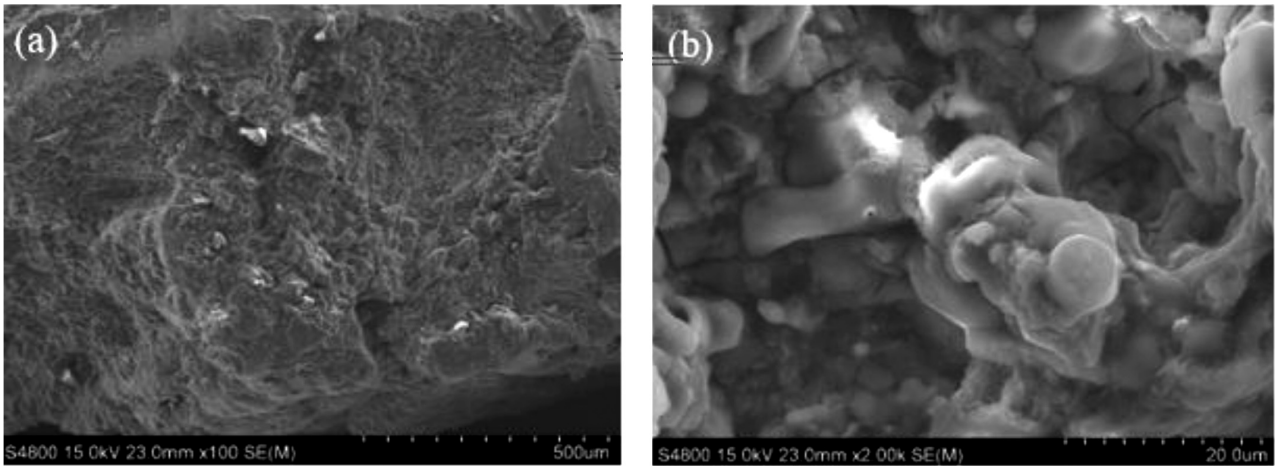

Figure 8: a) is the SEM scanning image of the fracture surface at a welding current of 16 kA, and b) is a magnified view of a region from (a)

5c. A careful observation of **Figure 3.6** reveals that at a welding current of 12 kA, the failure mode is interface failure with a metallic luster and a relatively smooth fracture surface. However, when the current is increased to 14 kA and 16 kA, the failure mode shifts to weld nugget pull-out failure, and these specimens exhibit larger nugget sizes with observable cavities.

Taking the samples with 12 kA and 14 kA as examples, combined with the SEM scanning images of the crack surfaces shown in **Figures 6a** and **6b** and **Figures 7a** and **7b**, the fracture morphology typically exhibits a river-like pattern, with a notably smooth surface. Thus, at welding currents of 12 kA and 14 kA, the fracture surfaces show brittle fracture characteristics.

At the onset of fracture, the joint has not yet experienced twisting. Under tensile normal stress, the stress is distributed evenly in this region. Under shear stress, holes are elongated in the shear direction, leading to crack formation. Observing the fracture morphology in **Figures 8a** and **8b**, which shows cracks traversing the grains, confirms the brittle fracture at 16 kA.

3.3 The hardness of spot weld joints

Figure 9 shows detailed microhardness testing results for the fusion zone, heat-affected zone, and base material of three sample groups.[26] The data indicate that the microhardness of the fusion zone is the highest among these regions. As the observation position moves from the fusion zone towards the heat-affected zone along the diameter, a gradual decrease in microhardness is noted.[27–29] This observation reveals a significant microhardness distribution feature, with the fusion zone exhibiting the highest microhardness, clearly surpassing that of the heat-affected zone and base material. This finding suggests that during spot welding, the fusion zone undergoes high-temperature melting and rapid cooling, resulting in a fine metal microstructure that enhances its hardness. The hardness distribution also indicates that the vulnerable area of the spot weld is mainly located in the heat-affected zone. In this experiment, the fusion zone's hardness was highest at a welding current of 16 kA and lowest at 12 kA. Future improvements can focus on adjusting the welding parameters and optimizing the welding materials to reduce brittleness in the heat-affected zone, thereby enhancing the overall performance and the lifespan of spot welds. This research advances welding technology and industrial development.

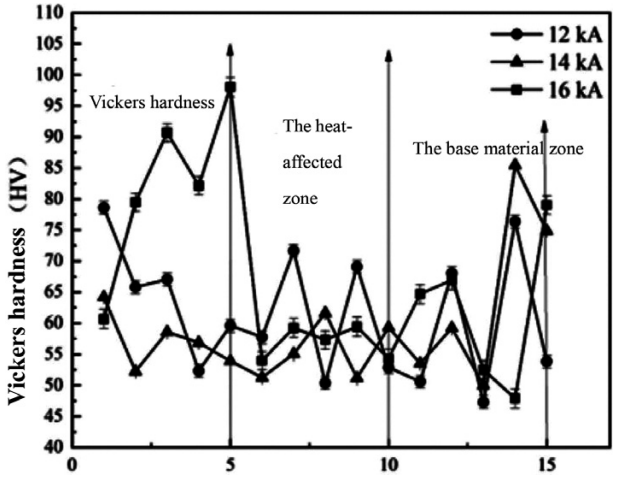

Figure 8: Hardness distribution map of different regions of the joint under different currents

The research indicates that factors such as the weld nugget diameter, Vickers hardness, second phase, fracture morphology, and shear tensile strength are crucial in determining the performance of magnesium alloys. In this study, both the deformation during welding and the heat input (primarily influenced by current parameters) together determine the ultimate mechanical performance of the weld. Specifically, the relationship between weld nugget diameter and tensile mechanical properties was examined. Generally, a larger nugget diameter results in a stronger weld, thereby improving tensile properties. This is due to a larger nugget diameter allowing more metal to melt and solidify, forming a stronger bond. In the weld samples, the Mg-7Sn-1Ca resistance spot welds exhibited a coarse dendritic structure in the heat-affected zone. This dendritic structure led to a significant decrease in microhardness in the heat-affected zone. There is a negative correlation between the shear load and the width of the CDZ, where a wider CDZ results in a lower shear load capacity. At 16 kA current, spattering and cracking occurred in the weld joints, reducing mechanical performance. As the nugget area moved toward the heat-affected zone along the diameter, a gradual decrease in microhardness was observed. The base material was slightly harder than the heat-affected zone, making the latter the most vulnerable.

5 CONCLUSIONS

This article starts with the potential application of Mg-Sn alloys and designs a preparation scheme for magnesium alloys, which is strictly followed to ensure the accuracy of the experimental results. After preparation, a detailed analysis of the microstructure and mechanical properties of Mg-7Sn-1Ca alloy weld joints under resistance spot-welding conditions was conducted. By comparing the experimental data with theoretical predictions and through a series of rigorous experiments and analyses, some important conclusions can be drawn.

(1) As the CDZ (nugget diameter) increases, the maximum shear load capacity of the weld joint decreases. Specifically, welding at a current of 16 kA introduces defects such as spattering and cracking, leading to significant deterioration in the joint's mechanical performance. The microhardness decreases gradually from the center of the nugget towards the heat-affected zone.

(2) The optimal spot-welding parameters under this experiment are a current of 14 kA, pressure of 1 kN and

welding time of 0.4 s. Under these conditions, the sample's weld nugget diameter is the largest at 2.5 mm, with higher nugget hardness and the best tensile performance, with a test force of 1.0295 kN.

Acknowledgements

The authors acknowledge the Natural Science Foundation of Fujian Province 2021J05232 and Science and Technology Planning Project of Longyan2021LYF9012.

6 REFERENCES

[1] J. L. Cheng , D. H. Cheng, A. T. Qi, et al. Microstructure and mechanical properties of resistance spot welding joint with high entropy alloy powder AZ31B magnesium alloy/304 stainless steel J. Materials Engineering, 52 (**2024**), 146–152

[2] P. F. Zhao, Q. Y. Zhang, W. W. Gu et al. Resistance spot welding of aluminum alloy and magnesium alloy with tin sandwich J. Hot working process, 52 (**2023**), 33–38

[3] L. Zhang. Microstructure and Properties of Rare Earth Magnesium Alloy by Resistance Spot Welding D. Nanchang University, 2022

[4] Y. Cheng, T. Fang, H. Peng. A method for predicting the yield strength of AZ31 magnesium alloy bars processed by ambient extrusionJ. Materials Letters, 367 (**2024**) 02, 136–585

[5] Y. Lu. Study on Resistance Spot Welding Process and Nugget Formation Mechanism of Zn-Al-Mg Coated DC51D Steel D. Chongqing University, 2021

[6] L. Hu, Y. Z. Liu, C. Tu, et al. Effect of Nano-TiB-2 on Microstructure and Mechanical Properties of Laser Selective Melting 2024 Aluminum Alloy J. Powder Metallurgy Materials Science and Engineering, 24 (**2019**), 365–373

[7] J. Chen, Q. Y. Zhang. Effect of Ca Composite Addition on Microstructure and Properties of AZ81 Magnesium Alloy J. Casting, 67 (**2018**), 1099–1104

[8] H. Huang, L. Hou, H. Du, et al. Efficient dual defense: PDA-Cu coating for simultaneous corrosion resistance and antibacterial protection of Mg alloysJ. Corrosion Science, 233 (**2024**) 2, 103–112

[9] F. Z. Yang. Ultrasonic Vibration Assisted Welding of AZ41/AZ31B Magnesium Alloy D. Chongqing University, 2018

[10] X. J. Wang. Fatigue Crack Growth Behavior of AZ31B Magnesium Alloy and Its Friction Stirring Welding Joint D. Taiyuan University of Technology, 2018

[11] C. Q. Jia. Study on Electrodeposition of Magnesium in Ionic Liquids D. Shenyang Normal University, 2018

[12] Y. J. Ma. Effect of Y and CE Additions on Microstructure and Mechanical Properties of Mg-Li-Zn Alloy D. Harbin University of Engineering, 2018

[13] P. Shuai. Research on Nugget Forming and Mechanical Properties of AZ31B Magnesium Alloy Inverter Resistance Spot Welding Joint with Unequal Thickness D. Taiyuan University of Science and Technology, 2017

[14] T. Li, Y. Luo. Microstructure and Mechanical Properties of Resistance Spot Welding of AZ31B Magnesium Alloy J. Journal of Xihua University, Natural Science Edition, 33 (**2014**), 62–65

[15] F. Liu. Study on Preparation of Carbon Steel/Hypereutectic High Chromium Cast Iron Composites by Centrifugal Casting-Hot Rolling D. Kunming University of Technology, 2014

[16] G. Liu, Z. Yan, Y. Guo, et al. Effect of tissue fixatives on the corrosion of biomedical magnesium alloysJ. Heliyon, 10 (2024) 09, 30–86

[17] X. Tu, M. D. Li, J. M. Lin, et al., Study on Optimization of Process Parameters for Hot Melting Butt Welding of Polyethylene Pipeline for Gas J. Guangdong Chemical Industry, 40 (**2013**), 34–35

[18] L. Xu. Study on Powder Conveying and Process of Laser Powder Filling Welding for Galvanized Steel D. Hunan University, 2013

[19] F. H. Zhang, S. C. Wang, W. J. Qi et al., Effect of Al-5Zr-1B Master Alloy on Grain Refinement of Magnesium and Magnesium Alloys J. Materials Research and Application, 7 (**2013**), 25–30

[20] Y. F. Zhang. Numerical simulation of resistance spot welding of magnesium alloy AZ31B based on SYSWELD D. Hebei University of Science and Technology, 2010

[21] H. Zhou. Microstructure and Properties of AZ31 Magnesium Alloy FSW/TIG Welding Joint D. Dalian Jiaotong University, 2010

[22] F. Zhang. Study on Welding Mechanism of Magnesium Alloy Active Wire and Preparation of D. Dalian University of Technology, 2009

[23] G. Y. Zhang, F. F. Sui, J. Q. Miao et al. Effect of External Magnetic Field on Arc Morphology and Weld Quality of Magnesium Alloy TIG Welding J. Hot working process, 38 (**2009**), 113–115

[24] B. Lang. Study on Resistance Spot Welding of AZ31B Magnesium Alloy D. Jilin University, 2008

[25] Q. Wu. Study on microstructure and mechanical properties of resistance spot welded joints of magnesium alloy (AZ31B) D. Jilin University, 2008

[26] Z. X. Yao, D. P. Jiang, Z. G. Yang. Formation Mechanism and Preventive Measures of Crack in TIG Welding of AZ31B Magnesium Alloy J. Welding machine, 17 (**2006**), 54–56

[27] J. F. Huang, G. L. Song. Research Progress in Corrosion Testing and Analysis of Magnesium Alloys J. Chinese Journal of Corrosion and Protection, 44 (**2024**), 519–528

[28] H. Y. Wang. Study on Isothermal Oxidation Behavior of Mg-Y and Mg-Gd-Y Rare Earth Magnesium Alloys at 350 °C, D. Central South University, 2023

[29] C. Wang, G. Zhang, T. Luo, et al. Asymmetric and anisotropic quench sensitivity of ZA81M magnesium alloyJ. Journal of Alloys and Compounds, 992 (**2024**) 2, 174–639